

X-ray and optical properties of Broad Absorption Line Quasars in the Canada–France–Hawaii Telescope Legacy Survey

C. S. Stalin^{1*}, R. Srianand² and P. Petitjean³

¹*Indian Institute of Astrophysics, Block II, Koramangala, Bangalore 560034, India*

²*Inter-University Centre for Astronomy and Astrophysics, Post Bag 4, Ganeshkhind, 411007 Pune, India*

³*Institut d'Astrophysique de Paris, CNRS Université Pierre et Marie Curie, 98bis bd Arago, Paris 75014, France*

Accepted 1988 December 15. Received 1988 December 14; in original form 1988 October 11

ABSTRACT

We study the X-ray and optical properties of 16 Broad Absorption Line (BAL) quasars detected in a $\approx 3 \text{ deg}^2$ region common to the wide synoptic (W-1) component of the Canada–France–Hawaii Telescope Legacy Survey (CFHTLS) and the XMM Large Scale Structure survey (XMM-LSS). The BAL fraction is found to be 10% in full sample, 7% for the optical colour selected QSOs and as high as 33% if we consider QSOs selected from their IR colours. The X-ray detected non-BAL and BAL quasars have a mean observed X-ray-to-optical spectral slope (α_{ox}) of -1.47 ± 0.13 and -1.66 ± 0.17 respectively. We also find that the BAL QSOs have α_{ox} systematically smaller than what is expected from the relationship between optical luminosity and α_{ox} as derived from our sample. Based on this, we show, as already reported in the literature for quasars with high optical luminosities, our new sample of BAL QSOs have X-ray luminosity a factor of three smaller than what has been found for non-BAL QSOs with similar optical luminosities. Comparison of hardness ratio of the BAL and non-BAL QSOs suggests a possible soft X-ray weakness of BAL QSOs. Combining our sample, of relatively fainter QSOs, with others from the literature we show that larger balnicity index (BI) and maximum velocity (V_{max}) of the C IV absorption are correlated with steeper X-ray to optical spectral index. We argue that this is most likely a consequence of the existence of a lower envelope in the distribution of BI (or V_{max}) values versus optical luminosity. Our results thus show that the previously known X-ray weakness of BAL QSOs extends to lower optical luminosities as well.

Key words: surveys - galaxies: active - quasars: general - Xrays: general

1 INTRODUCTION

Broad Absorption Line (BAL) quasars are Active Galactic Nuclei (AGN) characterized by the presence of strong absorption troughs in their UV spectra. They constitute an observed fraction of about 10–15% of optically selected quasars (Reichard et al. 2003; Hewett & Foltz 2003). Recently, it has been shown that the actual BAL fraction could be higher as optical colour selection of QSOs may be biased against the BAL QSOs (see for example, Dai et al. 2008; Shankar et al. 2008; Urrutia et al. 2009; Allen et al. 2010). The BALs are attributed to material flowing outwards from the nucleus with velocities of 5000 to 50000 km/s (Green et al. 2001). These quasars are classified into three subclasses based on the material producing the BAL troughs. High ion-

ization BAL quasars (HiBALs) have broad absorption from C IV, Si IV, N V and O VI. About 10% of BAL quasars also show, apart from their HiBAL features, broad absorption lines of lower ionization species such as Mg II or Al III and are called low-ionization BAL quasars (LoBALs). Finally, LoBALs with absorptions from excited states of Fe II or Fe III are called FeLoBALs (Wampler et al. 1995). BAL quasars in general have higher optical-UV polarization than non-BAL quasars, and the LoBALs tend to have particularly high polarization than HiBALs (Hutsemekers et al. 1998; Schmidt & Hines 1999; DiPompeo et al. 2010). LoBALs have a more reddened optical continuum compared to non-BAL and HiBAL QSOs (Becker et al. 2000; Sprayberry & Foltz 1992), thereby suggesting the presence of larger amounts of dust in them. In X-rays too, LoBALs have higher absorbing column densities than HiBALs (Green et al. 2001; Gallagher et al. 2002).

* E-mail: stalin@iiaap.res.in

The dichotomy between BAL and non-BAL quasars is often thought to be a consequence of orientation. The similarity between the optical/UV emission lines and continuum properties of BAL and non-BAL quasars (Weymann et al. 1991; Reichard et al. 2003) supports a scenario where the observed fraction of BAL quasars corresponds to the covering fraction of a wind that could be present in all AGN. Earlier spectropolarimetric observations too support this orientation scheme (Goodrich & Miller 1995; Hines & Wills 1995). However, recent spectropolarimetric observations of radio-loud BALs do not favour the orientation dependent scheme for the BAL phenomenon (DiPompeo et al. 2010). On the other hand, Allen et al. (2010) found a strong redshift dependence of the C IV BAL quasar fraction. They conclude that the BAL phenomenon cannot be due to an orientation effect only. Alternative to the orientation scheme it is argued that the observed BAL quasar fraction could correspond to the intrinsic fraction of quasars hosting massive nuclear winds, thereby tracing an evolutionary phase of the AGN lasting $\approx 10\text{--}15\%$ of their lives (Hazard et al. 1984; Becker et al. 2000; Giustini et al. 2008). In this scenario, the large amounts of gas and dust surrounding the central source should lead to enhanced far-infrared and sub-millimeter emission in BAL quasars with respect to non-BAL quasars (Giustini et al. 2008). However, sub-millimeter studies found no (Willott et al. 2003) or little (Priddey et al. 2007) differences among the two populations. Also, the mid-IR properties of BAL and non-BAL quasars of comparable luminosities are indistinguishable (Gallagher et al. 2007). BAL quasars are predominantly radio-quiet while few radio-loud BAL quasars are also known (Becker et al. 2000; Brotherton et al. 2005).

Although radiative acceleration could be the main driving mechanism in BAL quasars (Arav et al. 1994; Srianand et al. 2002), we still do not have a clear picture of the physics of outflows/winds in BALs. X-ray observations can help constrain the physical mechanisms at play in BAL quasar outflows and the different scenarios proposed (Giustini et al. 2008). Since the ROSAT survey, BAL quasars which are radio-quiet, have been known to have faint soft X-ray to optical luminosity ratio (Green et al. 1995; Green & Mathur 1996). Their X-ray luminosity is typically 10–30 times lower than expected from their UV luminosity, qualifying them as soft X-ray weak objects (Laor et al. 1997). This implies that the soft X-ray continuum of BAL quasars is either (a) strongly absorbed by highly ionized material or (b) intrinsically under luminous. Given the extreme absorption evident in the ultraviolet, this soft X-ray faintness was assumed to result from intrinsic absorption in BAL material of high column density, typically $N_{\text{H}} > 10^{22} \text{ cm}^{-2}$ (Gallagher et al. 2006, hereafter G06; Green et al. 1995; Green et al. 2001; Brotherton et al. 2005; Fan et al. 2009; Gibson et al. 2009). However, it has also been argued that intrinsic X-ray faintness cannot be ruled out as the cause for their observed X-ray weakness (Sabra & Hamann 2001; Mathur et al. 2000; Gupta et al. 2003, Giustini et al. 2008; Wang et al. 2008; Ghosh & Punsly 2008). Radio-loud BAL quasars are also found to be X-ray weak when compared with radio-loud non-BAL quasars of similar UV/optical luminosities (Miller et al. 2009).

X-ray spectral analysis of BAL quasars considering neutral and ionized absorbers are found to yield low neutral

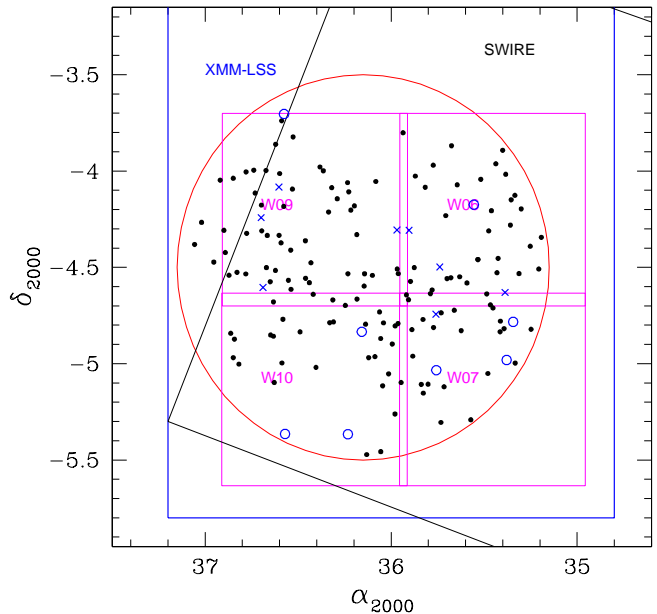


Figure 1. Layout of the field used to select quasars in this study. The XMM-LSS and SWIRE regions are delineated. W06, W07, W09 and W10 are the four pointings of CFHTLS and the large circle is the ~ 3 square degrees region searched for quasars in this work. The quasars are marked as filled circles, the BAL quasars detected in X-ray are shown as crosses and the BAL quasars undetected in X-rays are shown as open circles.

hydrogen ($N_{\text{H}} < 10^{21} \text{ cm}^{-2}$) and high ionized hydrogen ($N_{\text{H}}^i > 10^{21} \text{ cm}^{-2}$) column density respectively (Giustini et al. 2008; Streblyanska et al. 2010). It thus seems that the inferred N_{H} values depends on (a) the ionization state of the gas in our line of sight to the BAL quasar and (b) the absorber either fully or partially covering the X-ray source. Here, we investigate the issue of the X-ray weakness of BAL quasars using a new sample of quasars selected in the Canada–France–Hawaii Telescope Legacy Survey (CFHTLS¹) and overlapping the XMM Large Scale Structure survey (XMM-LSS) and the Spitzer Wide-area Infrared Extragalactic (SWIRE) Survey with the aims of (i) identifying a homogeneous sample of BAL quasars from a parent quasar sample and (ii) of studying the X-ray nature of those identified BAL quasars. The sample has been selected without a prior knowledge of the BAL nature of the objects. This paper is organized as follows. The data set used and the observations are described in Sect. 2. Identification of BAL quasars is given in Sect. 3. Results of the analysis are presented in Sect. 4 and the conclusions are drawn in Sect. 5. Throughout this paper we adopt a cosmology with $H_0 = 70 \text{ km s}^{-1} \text{ Mpc}^{-1}$, $\Omega_{\text{m}} = 0.27$ and $\Omega_{\Lambda} = 0.73$.

2 DATASET

The optical data set used in this work is from the wide Synoptic component (W-1) of CFHTLS. CFHTLS images

¹ <http://www.cfht.hawaii.edu/Science/CFHTLS/>

are available in five optical bands (u^* , g' , r' , i' and z') down to $i'_{AB} = 24$ mag. The field has been observed in the course of the XMM-LSS. Centered at ($\alpha_{2000} = 37.5$ deg, $\delta_{2000} = -5$ deg), the XMM-LSS (Pierre et al. 2004) is a medium depth large area X-ray survey designed to map the large scale structures in the nearby universe. The catalog for the first 5.5 square degrees (pertaining to 45 XMM pointings) observed in the 0.5–2 and 2–10 keV bands, listing sources above a detection likelihood of 15 in either bands, was released by Pierre et al. (2007). Also, overlapping the XMM-LSS and CFHTLS fields is the SWIRE Survey (Lonsdale et al. 2003).

We are in the process of carrying out optical spectroscopic identification of quasar candidates selected in about 10 square degrees in the W-1 region. Some regions of W-1 also have coverage from XMM-LSS and SWIRE. Therefore several selection criteria were adopted to select quasar candidates namely: (i) optical colour-colour criteria similar to that used in SDSS (Richards et al. 2002), (ii) IR colour-colour criteria following Stern et al. (2005) and (iii) optical SED matching using the photometric redshift code *hyperz* (Bolzonella, Miralles & Pellò 2000). Our final list of quasar candidates in W-1 thus consists of (a) candidates selected both by optical colour and template matching criteria, (b) candidates selected by optical colour but missed by template matching method, (c) candidates selected by optical template matching method but missed by optical colour selection (d) candidates selected by IR colour selection but missed in optical selection and (e) all XMM sources having optical counterparts, but not selected through (a),(b),(c)and (d). Our candidate selection was limited to sources brighter than $g' < 22$ mag. A complete description of our procedure of quasar candidate selection as well as the results of the quasar selection efficiency will be discussed in a forthcoming paper (Stalin et al. *in preparation*) when our complete quasar survey will be reported. Our main aim here is to understand the X-ray and optical properties of BAL quasars. Thus, for this work we have considered only ≈ 3 square degree region in W-1, which has both optical and X-ray imaging observations. This region is shown as a large circle in Fig. 1. Also, marked on this figure are the regions covered by the XMM-LSS and SWIRE.

Optical spectroscopic observations of the quasar candidates selected in the ≈ 3 square degrees circular region shown in Fig. 1 were carried out with the AAOmega system (Sharp et al. 2006) on the 3.9 m AAT, during two observing runs in September 2006 and 2007. The field of the camera has a diameter of 2 degree and was centered at $\alpha_{2000} = 36.15$ deg and $\delta_{2000} = -4.50$ deg (see Fig. 1). The 580V and 385R gratings were used, respectively, in the blue and red arms of the spectrograph, thereby simultaneously covering the wavelength range 3700–8800 Å, and delivering a spectral resolution of $R \sim 1300$. The total integration time ranged from 30 min to 3 hours depending on the brightness of the candidates.

Spectroscopic data reduction was performed using the AAOmega's data reduction pipeline software DRCONTROL. The two dimensional images were flat fielded, and the spectra were extracted (using a gaussian profile extraction), wavelength calibrated and combined within DRCONTROL. Redshifts were derived using the AUTOZ code (kindly provided to us by Scott Croom). Individual QSO

spectra were manually checked to confirm the correctness of the redshift. Further details of the observations and reductions can be found in Stalin et al. (2010).

A total of 159, $z_{em} > 1.5$, new quasars were identified from the AAT observations in ≈ 3 deg². They are shown as filled circles in Fig. 1. This is the sample we use here to investigate the X-ray properties of BAL and non-BAL quasars. Note that the above redshift cut-off is necessary in order to observe the C iv $\lambda 1549$ BAL feature in the spectral range 3800–8800 Å. Out of these 159 quasars, 120 were primarily selected based on optical colour selection without any prior knowledge of X-ray emission, 12 sources were selected based on their IR colour (also without any knowledge of X-rays) from the SWIRE survey but were missed by our optical selection and 27 sources were selected from the XMM source list through the presence of X-ray emission. We find 72% (i.e. 86 quasars out of 120) of the optically selected quasars are also detected in XMM. However, only 33% (i.e., 4 quasars out of 12) of the IR only selected candidates are detected by XMM. All of the 120 optically colour selected quasars were detected by SWIRE in one of the five IR bands. However, only 78 of these 120 sources have IR flux values in all the four IR bands so that IR selection criteria can be applied to them. Of these 78, 77 are also IR colour-colour selected. The average $u' - g'$ and $g' - r'$ colours of the 12 IR only selected quasars are redder than that of the 120 optically colour selected quasars.

3 IDENTIFYING BALS

From our sample of 159 quasars, we initially identified quasars with broad C iv absorption close to the emission redshift by eye. We then for these quasars calculated the balnicity index (BI) as defined by Weymann et al. (1991)

$$BI = - \int_{25000}^{30000} \left[1 - \frac{f(v)}{0.9} \right] C dv. \quad (1)$$

Here, $f(v)$ is the continuum-normalized flux at a velocity v (in km s⁻¹) defined with respect to the quasar rest frame. The dimensionless value C is initially set to zero. It is set to 1.0 whenever the quantity in brackets has been continuously positive over an interval of 2000 km s⁻¹. Traditionally BAL quasars are defined as quasars with BI > 0. We fitted a smooth continuum to these quasar spectra using the method similar to the one described in Trump et al. (2006). The normalized spectrum is used to measure BI. We also simultaneously estimated V_{max} , the maximum outflow velocity at which $f(v)$ is 0.9. The properties of the 16 new BAL (all HiBALS) quasars with BI greater than 100 km s⁻¹ are summarized in Table 1. They are shown as crosses (BALS detected in X-rays in XMM-LSS) and open circles (BALS un-detected in X-rays in XMM-LSS) in Fig. 1. Of these 16 BAL quasars, we have Mg II coverage for 6 BAL quasars. None of these 6 BALS are found to be LoBALS. This is not surprising, as we would expect to see 1.6 LoBALS if all the 16 BALS had Mg II coverage in their spectra, as only 10% of optically selected BALS are known to be LoBALS.

We find a BAL quasar fraction $f_{BAL} = N(BAL)/N(Total) \approx 10 \pm 3\%$ in our sample. If we restrict ourselves to the optical colour selected quasars we find $8 \pm 3\%$ of them are BAL quasars. We also find $7 \pm 5\%$

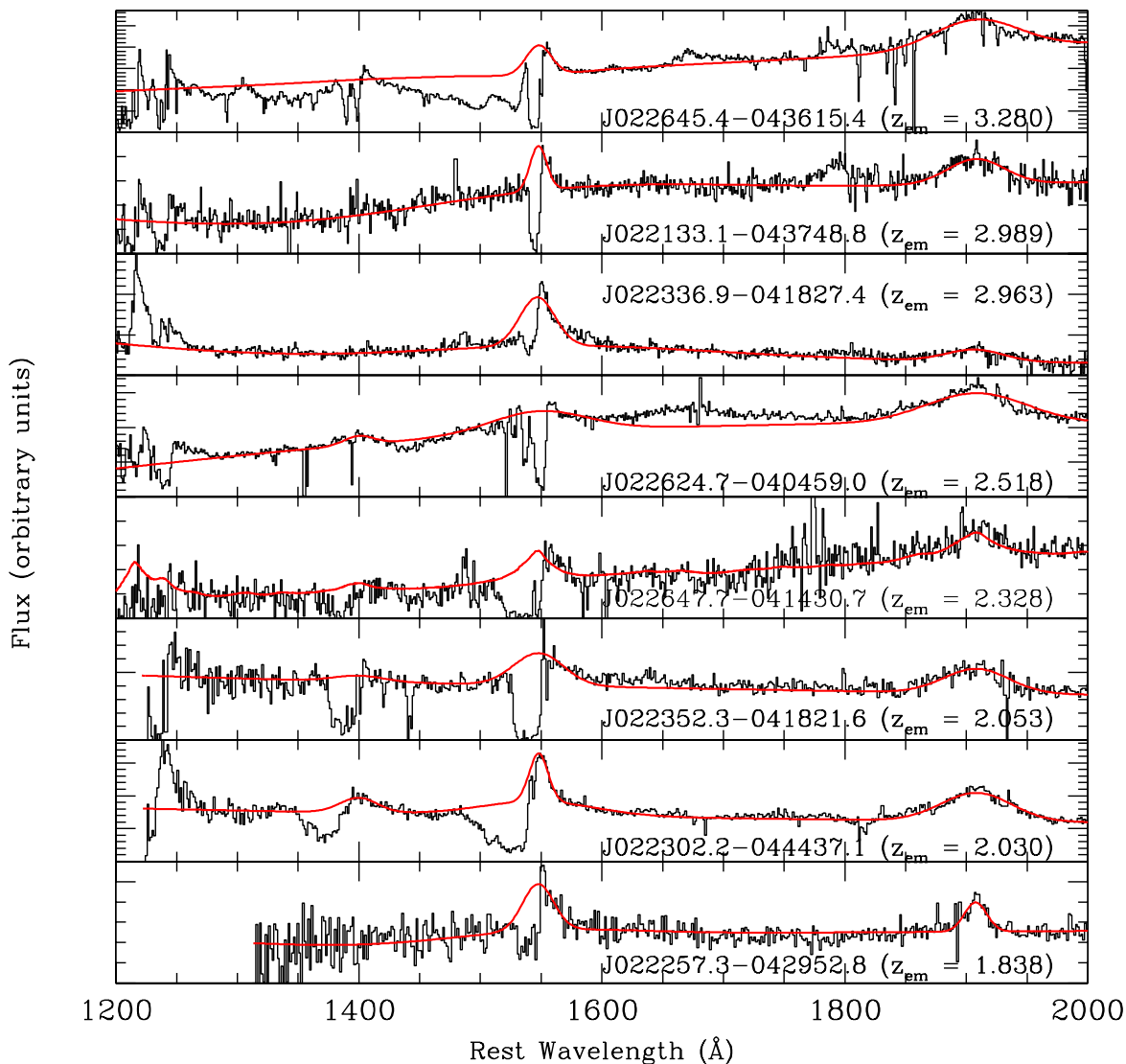


Figure 2. The rest frame spectra of BAL quasars detected by XMM in our sample. The best fitted continuum is over plotted.

of the XMM selected quasars to be BAL quasars. This is consistent with the rate found for the optical colour selected candidates. There are 12 quasars which are selected via IR colour selection but are not part of our optical colour selection. Out of these 12 quasars, 4 are found to be BAL quasars. We thus find a BAL detection rate of $33 \pm 19\%$ among the IR only selected quasars.

In our sample of optically selected quasars, the observed BAL quasar fraction is very similar to the fraction 10–15% reported in the literature from optically selected quasar samples (see Weymann et al. 1991, Hewett & Foltz 2003; Reichard et al. 2003; Tolea, Krolik & Tsvetanov 2002; Trump et al. 2006, Knigge et al. 2008, Gibson et al. 2009). However, the BAL quasar fraction found in optically selected sample could not represent the true BAL fraction. This is because optical surveys will miss BAL quasars as their optical broad band colours are affected by reddening in their UV spectra

and large absorption in their BAL troughs. This is clearly evident in the higher BAL quasar fraction of $23 \pm 3\%$ reported by Dai et al. (2008) in the 2MASS selected quasars. When Hewett & Foltz (2003) considered the effect of reddening in their BAL quasars sample, they found a BAL quasar fraction of 22% similar to that of Dai et al. (2008). High BAL quasar fraction is also claimed in the samples selected based on radio emission (see Shankar et al. 2008; Urrutia et al. 2009). Interestingly, this is also consistent with the higher BAL quasar fraction we find among the objects selected from IR colours only. Note that Dai et al. (2008) argued that the selection based on optical colours has significant selection biases against BAL quasars, and the BAL quasar fraction in NIR colour selected sample more accurately reflects the true fraction of BAL quasars. Indeed, Allen et al. (2010) have shown that, when the incompleteness related to the BAL identification in the SDSS spectrum and the colour

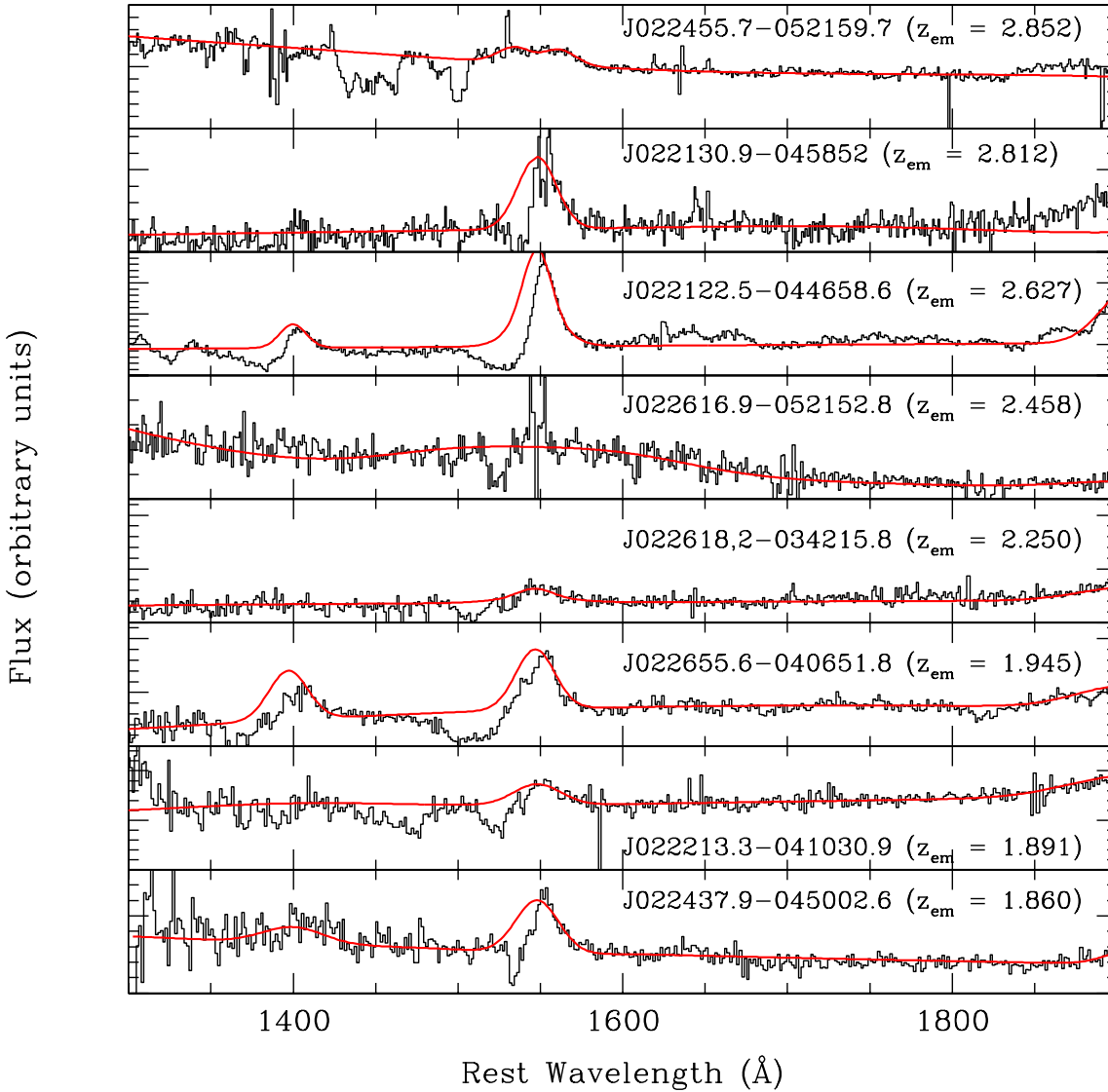


Figure 3. The rest frame spectra of BAL quasars in our sample without X-ray detection. The best fitted continuum is over plotted.

selection method used to identify QSOs were taken into account, the actual BAL fraction can be as high as 41 ± 5 per cent instead of 8.0 ± 0.1 per cent found from the SDSS sample.

Of the 16 BAL quasars in our sample, 8 are detected in XMM-LSS ($50 \pm 22\%$). Even if we restrict the sample to the colour selected objects, we find equal numbers of BAL quasars with and without detectable X-ray emission (i.e. 50%). The spectra of the 8 BAL quasars that are detected by XMM in XMM-LSS are shown in Fig. 2. Fig. 3 shows the spectra of the remaining 8 BAL quasars that are not detected in XMM-LSS. Our X-ray detection rate is slightly lower than the $77 \pm 20\%$ reported by G06, $74 \pm 13\%$ reported by Gibson et al. (2009) and $63 \pm 16\%$ reported by Fan et al. (2009). However, within uncertainties our value matches well with that from previous studies. There are two main differences between our study and the above listed studies.

Firstly, our sample is optically selected and then correlated with XMM-LSS, thereby, BAL and non-BAL quasars have similar X-ray flux limits and secondly, the quasars in our study are typically fainter than that used in the other three studies (see Fig. 5). It is also interesting to note that on an average, objects in the sample of G06 are optically more luminous than those of Fan et al. (2009). Similarly, objects in our sample are systematically fainter than the sample considered by Fan et al (2009).

There are seven radio-loud quasars in our sample (see Table 5 of Stalin et al. 2010). None of them is a BAL quasar. Using the BAL fraction found by Shankar et al (2008) for radio selected quasars, we should expect 1.5 radio-loud BAL quasars.

4 PROPERTIES OF BAL QUASARS IN OUR SAMPLE

4.1 Optical-to-X-ray spectral index (α_{ox})

The broad band spectral index α_{ox} is generally used to quantify the relative UV to X-ray power of the quasar. We estimated α_{ox} for each of the spectroscopically identified AGN in our sample. For this we have converted the observed i' -band magnitudes to fluxes following the definition of the AB system (Oke & Gunn 1983)

$$S_{i'} = 10^{-0.4(m_{i'} + 48.60)}. \quad (2)$$

where $S_{i'}$ and $m_{i'}$ are respectively the flux and magnitude in the i' -band. The luminosity at the frequency corresponding to 2500 Å in the rest-frame is calculated following Stern et al. (2000)

$$L_{\nu_1} = \frac{4\pi D_l^2}{(1+z)^{1+\alpha_o}} \left(\frac{\nu_1}{\nu_2}\right)^{\alpha_o} S_{\nu_2} \quad (3)$$

where ν_2 is the observed frequency corresponding to the i' -band, S_{ν_2} is the observed flux in i' -band, ν_1 is the rest-frame frequency corresponding to 2500 Å and D_l is the luminosity distance. An optical spectral index $\alpha_o = -0.5$ (Anderson et al. 2007) is assumed ($S_\nu \propto \nu^\alpha$). The luminosity at 2 KeV in the rest frame is obtained using a similar equation as Eq. 3, assuming a X-ray spectral index of $\alpha_x = -1.5$ (Anderson et al. 2007).

Thus, the broad band spectral index α_{ox} is obtained as

$$\alpha_{\text{ox}} = \frac{\log(L_{2\text{KeV}}/L_{2500\text{\AA}})}{\log(\nu_X/\nu_{\text{opt}})} \quad (4)$$

Here $L_{2\text{KeV}}$ and $L_{2500\text{\AA}}$ are the rest frame monochromatic luminosities (in $\text{erg s}^{-1} \text{Hz}^{-1}$) at $\nu_X = 2\text{KeV}$ and ν_{opt} corresponding to 2500 Å respectively.

Fig. 4 shows the distribution of observed α_{ox} (not corrected for intrinsic and Galactic absorption) for the sample of XMM detected non-BAL and BAL quasars. The BAL quasars have systematically lower values of α_{ox} compared to the non-BAL quasars. We find a mean $\alpha_{\text{ox}} = -1.47 \pm 0.13$ and -1.66 ± 0.17 for the XMM detected non-BAL and BAL quasars respectively. In our sample, the upper limits of α_{ox} derived for the XMM un-detected BALs are towards the lower end of the distribution of α_{ox} found for XMM detected non-BAL quasars as can be seen in Fig. 4.

We now compare our results with other BAL quasar studies. In Fig. 5, we show the distribution of $L_{2500\text{\AA}}$ luminosity and α_{ox} for our sample of BAL quasars as well as other quasar samples published in literature. Objects in our sample are systematically fainter than those in the published samples namely G06, Fan et al. (2009), Giustini et al. (2008) and Gibson et al. (2009). The α_{ox} distribution of our sample has some overlap with Fan et al. (2009), Giustini et al. (2008) and Gibson et al. (2009) samples, but is offset from the distribution of G06. G06 found a median α_{ox} of -2.20 , which is much smaller than that found by Fan et al. (2009), Giustini et al. (2008) and Gibson et al. (2009). The objects in the G06 sample are luminous and the low value of α_{ox} found might be due to the dependence of α_{ox} on luminosity reported by various authors (Green et al. 2009, Steffen et al. 2006, Just et al. 2007). Recently, for CFHTLS quasars, Stalin et al. (2010) found a dependence of α_{ox} on $L_{2500\text{\AA}}$ and is given by

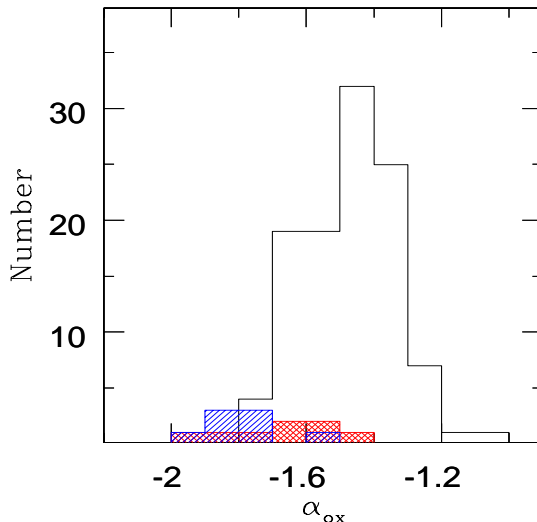


Figure 4. Distributions of α_{ox} in our sample. The solid histogram is for the XMM detected non-BAL quasars. The hashed histogram is for the XMM detected BAL quasars and the shaded histogram shows the upper limits of α_{ox} for the X-ray un-detected BAL quasars.

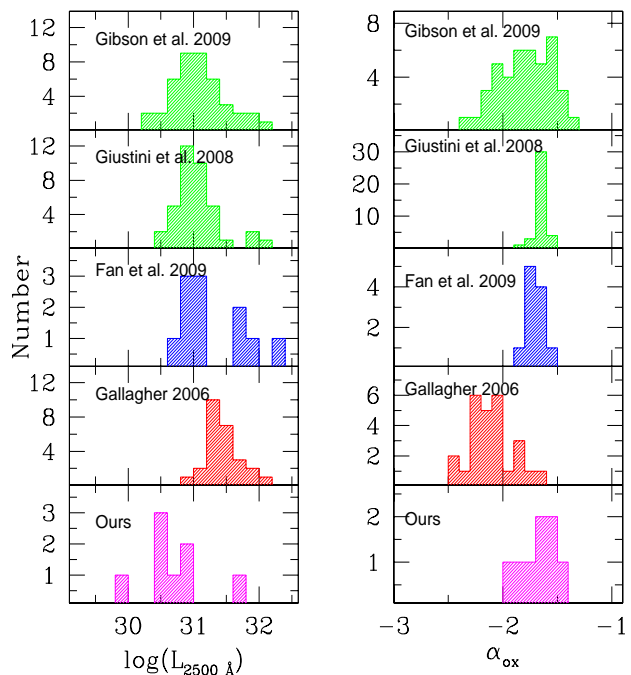


Figure 5. Distribution of the monochromatic luminosity at 2500 Å (left panel) and α_{ox} (right panel) in several BAL quasar samples. The references from where the samples are taken are given in each panels.

$$\alpha_{\text{ox}} = (-0.065 \pm 0.019) \log(L_{2500}) + (0.509 \pm 0.560). \quad (5)$$

This relation is in agreement to that found by Green et al. (2009), however, flatter than the value found by Steffen et al. (2006) and Just et al. (2007). To overcome this dependency of α_{ox} on $L_{2500\text{\AA}}$ luminosity, we study the distribution of $\Delta\alpha_{\text{ox}}$ values for our sample. For calculating $\Delta\alpha_{\text{ox}}$ values, we opted to use the relation between α_{ox} and $L_{2500\text{\AA}}$

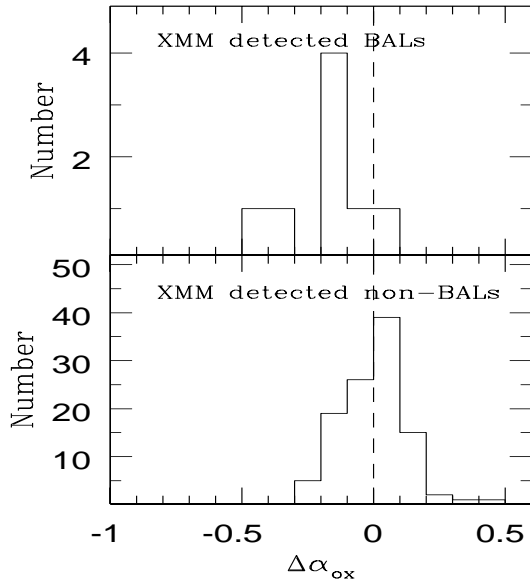


Figure 6. Distributions of $\Delta\alpha_{\text{ox}}$ in our sample. The top panel is for XMM detected BAL quasars and the bottom panel is for the XMM detected non-BAL quasars.

obtained by Stalin et al. (2010) for the CFHTLS quasars. $\Delta\alpha_{\text{ox}}$ is defined as the difference between the observed α_{ox} and $\alpha_{\text{ox}}(L_{2500\text{\AA}})$ calculated using Eq. 5 given the optical luminosity of the object. This gives an estimate of how the X-ray luminosity of a BAL quasar differs from that of a typical non-BAL quasar of the same $L_{2500\text{\AA}}$. For BAL quasars culled from literature, $\Delta\alpha_{\text{ox}}$ was recalculated using Eq. 5. The distributions of $\Delta\alpha_{\text{ox}}$ for our sample of BAL and non-BAL quasars are shown in Fig. 6. In the case of XMM detected non-BAL quasars, $\Delta\alpha_{\text{ox}}$ is found to be distributed symmetrically around zero. On the contrary, the distribution of $\Delta\alpha_{\text{ox}}$ for XMM detected BAL quasars is offset from zero. The average $\Delta\alpha_{\text{ox}}$ for XMM detected non-BAL and BAL quasars are 0.005 ± 0.119 and -0.169 ± 0.161 respectively. Using Eq. 5 we can say that $\Delta\alpha_{\text{ox}}$ of -0.169 corresponds to an X-ray luminosity weaker by a factor of ~ 3 with respect to typical non-BAL quasars of the same $L_{2500\text{\AA}}$. Thus, in our sample, BAL quasars appear to be X-ray weak compared to their non-BAL counterparts. This is similar to what some previous studies have reported (G06; Fan et al. 2009; Gibson et al. 2009).

4.2 Correlation between X-ray and UV properties

Models of BAL outflows based on radiation driven flows predict a correlation between the outflow velocity (V_{max}) and the quasar luminosity (Arav et al. 1994). The transfer of photon momentum depends on the column density and the ionization state of the absorbing gas. The ionization state of the BAL outflow very much depends on the optical to soft X-ray spectral energy distribution of the ionizing continuum (Srianand & Petitjean 2000; Gupta et al. 2003). In order for an efficient transfer of radiative momentum to the absorbing gas it is important that the gas is not over-ionized despite being very close to the central engine (see Proga et al. 2000). This can be achieved if there is a highly ionized (not seen

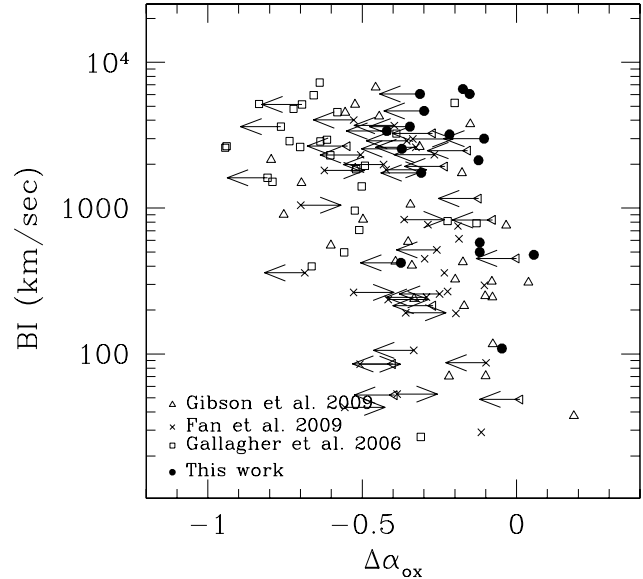


Figure 7. Correlation between BI and $\Delta\alpha_{\text{ox}}$ for various BAL quasar samples taken from the literature.

in UV absorption) gas component at the base of the flow that shields X-rays from the UV absorbing gas (Murray & Chiang 1995). In such a scenario one would expect the properties of the UV absorbing gas to be related to the properties of the X-ray absorbing gas at the base of the same flow. We therefore investigate correlations between the kinematical properties of UV absorptions (V_{max} and BI) with $\Delta\alpha_{\text{ox}}$, an indicator of X-ray absorption, and $L_{2500\text{\AA}}$. For these statistical study we add to the new BAL quasars reported in this work, HiBALs from the literature. We have included 29 BAL QSOs from Gallagher et al. (2006), 38 BAL QSOs from Giustini et al. (2008), 42 BAL QSOs from Gibson et al. (2009) and 35 BAL QSOs from Fan et al. (2009). Thus our extended sample consists of 160 high ionization BAL QSOs. Even though our new BAL quasars constitute only 10% of the extended sample, it is significant to the statistical analysis as they are systematically fainter in optical luminosity than the ones from the literature.

In Fig. 7 we plot the balnicity index, BI, measured from the C IV absorption against $\Delta\alpha_{\text{ox}}$ for the enlarged sample of BAL quasars including our own 16 BAL quasars. In our sample two out of three of the BALs with BI greater than 5000 km/s show $-0.2 \leq \Delta\alpha_{\text{ox}} \leq -0.1$. However, among objects with $\text{BI} \geq 2000$ km/s, only 4 out of 10 BAL QSOs show X-ray detection, whereas 4 out of 5 objects with $100 \leq \text{BI} \leq 1000$ km/s are detected in X-rays. Thus there appears to be a tendency of QSOs with large BI values to be weaker in X-rays. Now, we explore this correlation in the extended sample discussed above. As BI values are not available for the objects in Giustini et al. (2008) the corresponding objects are not considered in the analysis. In Fig. 7 we plot $\Delta\alpha_{\text{ox}}$ against BI for all the remaining 122 objects in the combined sample. The Kendall - τ test as implemented in the Astronomy Survival Analysis (ASURV) package (Lavalley et al. 1992), that treats both upper and lower limits, gives a probability of $< 0.01\%$ that the two variables are uncorrelated (see Table. 2). This is consistent with a 99.95%

Table 1. Properties of BAL quasars in CFHTLS

RA h:m:s	Dec d:m:s	g' (mag)	α_{ox}	$\Delta\alpha_{\text{ox}}$	$L_{0.5-2\text{Kev}}$ (erg/s)	$L_{2\text{KeV}}$ (erg/sec/KeV)	$L_{2500\text{\AA}}$ (erg/sec/\AA)	z	V_{max} (km/sec)	Balnicity index
02:23:02.278	-04:44:37.057	19.89	-1.94	-0.466	43.50	26.36	30.82	2.03	10335.0	3200.0
02:23:52.537	-04:18:21.620	20.54	-1.83	-0.354	43.51	26.37	30.54	2.05	5701.0	2126.0
02:26:24.710	-04:04:59.075	19.84	-1.63	-0.119	44.48	26.77	31.00	2.52	19409.0	500.0
02:26:47.693	-04:14:30.763	20.78	-1.63	-0.152	44.06	26.34	30.59	2.33	8233.0	6065.0
02:26:45.443	-04:36:15.475	19.92	-1.72	-0.174	44.84	27.17	31.66	3.28	22440.0	6567.0
02:22:57.309	-04:29:52.856	21.68	-1.56	-0.119	43.66	25.90	29.96	1.84	4308.0	580.0
02:21:33.091	-04:37:48.852	21.45	-1.54	-0.047	44.45	26.76	30.77	2.99	3942.0	109.0
02:23:36.896	-04:18:27.431	21.24	-1.41	0.056	44.46	26.77	30.46	2.96	5569.0	479.0
02:24:55.759	-05:21:59.772	19.93	< -1.94	< -0.420	<43.86	<26.77	31.23	2.85	23766.0	3376.0
02:26:16.910	-05:21:52.820	20.39	< -1.79	< -0.309	<43.70	<26.59	30.65	2.45	6139.0	1742.0
02:22:13.311	-04:10:30.093	20.24	< -1.84	< -0.372	<43.43	<26.28	30.48	1.90	20640.0	2546.0
02:24:37.908	-04:50:02.572	20.42	< -1.85	< -0.375	<43.41	<26.26	30.46	1.87	4380.5	422.0
02:21:22.497	-04:46:58.606	20.43	< -1.84	< -0.345	<43.78	<26.67	30.88	2.63	10964.0	3620.0
02:26:18.182	-03:42:15.797	20.68	< -1.77	< -0.299	<43.61	<26.48	30.50	2.25	10053.0	4640.0
02:21:30.978	-04:58:52.086	21.95	< -1.56	< -0.105	<43.85	<26.75	30.22	2.81	4781.0	2996.0
02:23:01.742	-05:01:59.748	20.96	< -1.78	< -0.313	<43.46	<26.31	30.34	1.95	14430.0	6061.0

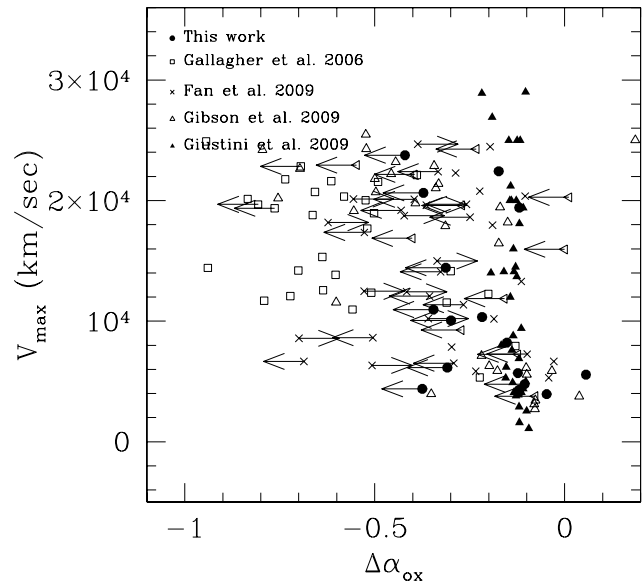
Table 2. Correlation analysis

Variables	Npoints	Kendall's τ	
		τ	Prob.(%)
V_{max} v/s $\Delta\alpha_{\text{ox}}$	160	5.243	<0.01
V_{max} v/s L_{2500} \AA	160	4.421	<0.01
BI v/s $\Delta\alpha_{\text{ox}}$	122	5.285	<0.01
BI v/s L_{2500} \AA	122	2.405	1.62
V_{max} v/s $\Delta\alpha_{\text{ox}}$	131 ¹	5.274	<0.01
V_{max} v/s L_{2500} \AA	131 ¹	3.954	0.01
V_{max} v/s $\Delta\alpha_{\text{ox}}$	93 ²	4.063	<0.01
V_{max} v/s L_{2500} \AA	93 ²	3.694	<0.01
BI v/s $\Delta\alpha_{\text{ox}}$	93 ¹	3.893	0.01
BI v/s L_{2500} \AA	93 ¹	0.624	0.53

¹ sample excluding data from G06.² sample excluding data from G06 and Giustini et al. (2008).

correlation found by Fan et al. (2009) between BI and $\Delta\alpha_{\text{ox}}$ (see also Gibson et al. 2009). From Fig. 7 it can be readily seen that most of the G06 sources have high BI occupying the top left corner of the diagram. To check if the derived correlation is dominated by the G06 sources, we applied the test without these sources. This time too, a correlation is noticed, with the Kendall τ test giving a probability of 0.01% that BI and $\Delta\alpha_{\text{ox}}$ are un-correlated (Table 2). This is mainly due to the fact that we have only upper limits on $\Delta\alpha_{\text{ox}}$ in most QSOs with BI > 1000 km/s.

Next we look for the correlations between V_{max} and $\Delta\alpha_{\text{ox}}$. There is no apparent trend between the two if we consider only our sample. The objects with upper limits on $\Delta\alpha_{\text{ox}}$ are spread over the whole V_{max} range. In Fig. 8 we plot V_{max} measured from the C IV absorption versus $\Delta\alpha_{\text{ox}}$ in the extended BAL quasar sample. The Kendall τ -test gives a probability of < 0.01% that the two variables are not correlated (Table 2). In the past, different samples have given different results for this correlation. Gallagher et al (2006) and Gibson et al. (2009) have found significant correlation between V_{max} and $\Delta\alpha_{\text{ox}}$ but this was not confirmed by Fan

**Figure 8.** Maximum outflow velocity, V_{max} versus $\Delta\alpha_{\text{ox}}$ for BAL quasar samples collected from the literature

et al. (2009) and Giustini et al. (2008). In the extended sample, even when we remove the points from Gallagher et al. (2006), we do find a very small Kendall probability ($P < 0.01\%$) that the two parameters are not correlated (see Table 2). If we remove points from Giustini et al. (2008), because they are not selected homogeneously, the Kendall τ test gives a probability < 0.01% that V_{max} and $\Delta\alpha_{\text{ox}}$ are uncorrelated.

It is a fact that the points in Figs. 7 and 8 appear to be scattered even though the Kendall test hints to the existence of a possible correlation between $\Delta\alpha_{\text{ox}}$ and kinematical parameters derived from the UV absorptions. This is mainly due to the paucity of points in the bottom left corner of both the plots.

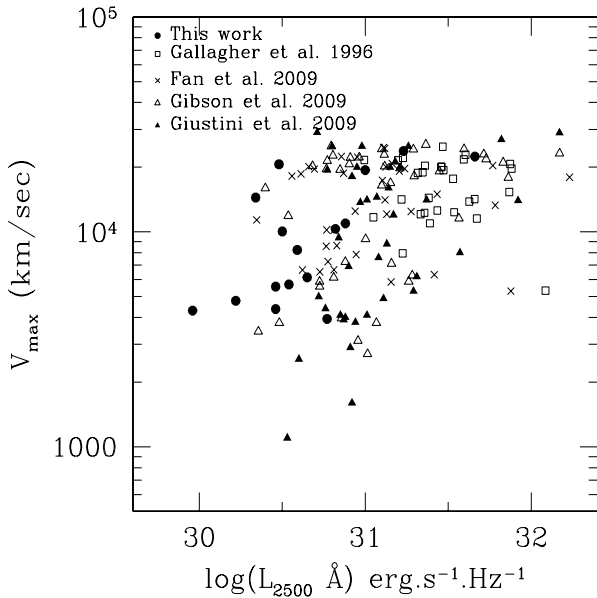


Figure 9. Maximum outflow velocity, V_{\max} , versus the monochromatic luminosity at 2500 \AA for various BAL quasars collected from the literature.

To explore this further, we plot in Fig. 9, V_{\max} measured from the C IV absorption against $L_{2500 \text{ \AA}}$. The Kendall τ -test gives a probability $< 0.01\%$ that V_{\max} and $L_{2500 \text{ \AA}}$ are not correlated both for the whole sample, sample excluding G06 sources, and the sample excluding both G06 and Giustini et al. (2008) sources. BAL quasars with high UV luminosities tend to have higher values of V_{\max} . While there is a large range in V_{\max} , for a given $L_{2500 \text{ \AA}}$ at $\log(L_{2500 \text{ \AA}}) < 31$, there is a lack of objects with $V_{\max} < 10^4$ km/s at the high luminosity end. Thus, there seems to be a lower envelope, the presence of which dominates the above correlation. This seems to be also the case when we plot BI against $L_{2500 \text{ \AA}}$ (see Fig. 10). The marginal correlation found between the two parameters may mainly be dominated by the absence of low BI sources at high optical luminosity. The above results are also consistent with that found by Ganguly et al. (2007)

A relationship between V_{\max} and luminosity is expected if the broad troughs originate in a radiatively driven wind. From the analysis of C IV absorptions in low- z Seyfert galaxies and high- z high luminosity QSOs, Laor & Brandt (2002) have shown that radiation-pressure force multiplier increases with luminosity (see also Ganguly et al. 2007). If true, this could explain the lower-envelopes seen here. However, our analysis also shows that there is a large scatter in BI and V_{\max} at any given luminosity. This probably means that even if radiation pressure is the main driver of the flow, other parameters are important such as the launching radius, the shape of the ionizing spectrum, the mass of the wind, the properties of the confining medium, etc..

4.3 X-ray hardness ratio

The hardness ratio is often the only spectral information that is possible to extract when the X-ray source is weak. We queried the observations available in the XMM-Newton

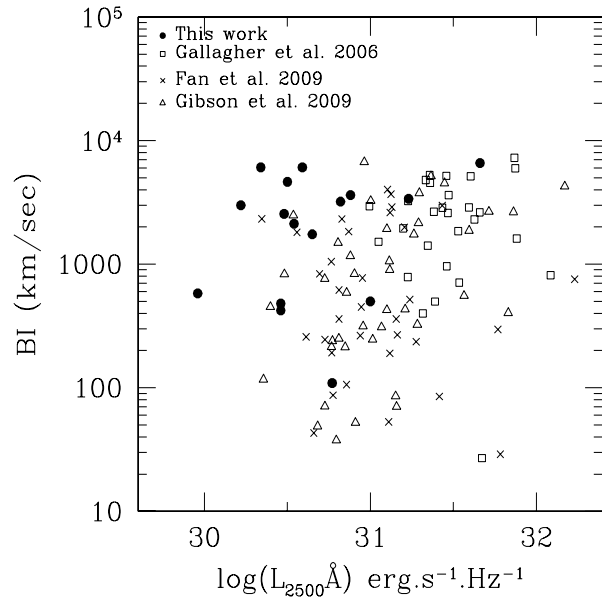


Figure 10. The balnicity index, BI, is plotted versus the QSO monochromatic luminosity at 2500 \AA for different samples of BAL quasars collected from the literature.

Science Archive version 6.0 (XSA) for all objects in our sample. For each observational ID, XSA provides the identified sources along with count rates and their associated errors in five energy bands. Thus, using XSA, we extracted the count rates for all our XMM-detected non-BAL and BAL quasars and estimated the hardness ratio (HR) between the soft (0.2–2 keV) and hard (2.0–10.0 keV) bands as:

$$HR = \frac{C(2.0 - 12.0\text{keV}) - C(0.2 - 2.0\text{keV})}{C(2.0 - 12.0\text{keV}) + C(0.2 - 2.0\text{keV})} \quad (6)$$

where $C(2.0-12.0 \text{ keV})$ and $C(0.2-2.0 \text{ keV})$ are, respectively, the count rates in the 2.0–12.0 keV and 0.2–2.0 keV bands. The errors in HR were estimated by propagating the errors in each individual energy bands. In our sample we have a total of 109 XMM detected non-BAL quasars. Of these the count rates were available for 106 sources. The average HR for these 106 sources is -0.61 ± 0.20 . Similarly, of the 8 XMM detected BAL quasars, good count rates are available for 7 XMM BAL quasars. The average HR for these 7 BAL quasars is -0.48 ± 0.20 . The HR distributions for the XMM detected BAL and non-BAL quasars are shown in Fig. 11. As the number of BAL quasars with X-ray detection is small, the trend of high HR in BAL quasars cannot be confirmed with any statistical significance.

4.4 X-ray spectral analysis

We also tried to perform a spectral analysis of archival XMM observations available for the 8 BAL quasars. For this we retrieved from XSA the original observational data file (ODF) for the 8 sources. These data were then reduced using the XMM Science Analysis Software (SAS) version 8.0.1. The original events files were filtered to retain only single and double pixel events ($\text{PATTERN} \leq 4$) as well as to retain only good quality events ($\text{FLAG} = 0$). From this filtered events file, time stamps having high background events were also

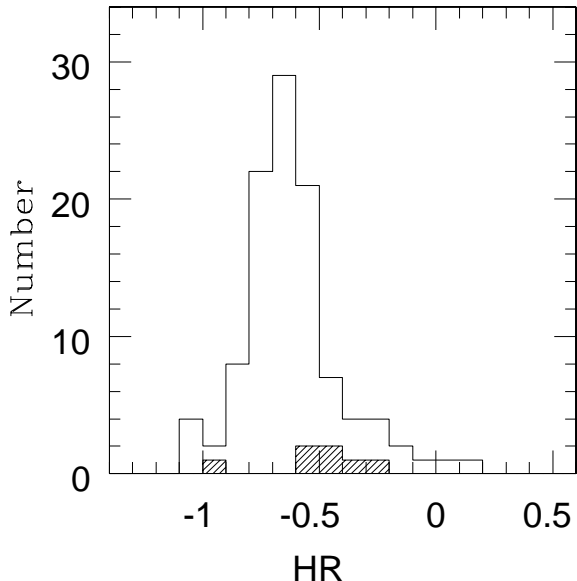


Figure 11. Distributions of the X-ray hardness ratio of the XMM-detected non-BALs (solid histogram) and BAL quasars (shaded histogram)

removed. From the final cleaned events file, individual source spectra were generated for each XMM detected BAL quasars with an extraction radius of 15–20'' for the source and the background region. The background region was extracted from noise free regions as close to the source as possible. Also, ancillary response file (ARF) and redistribution matrix file (RMF) at the position of the source were generated with the *argen* and *rmfgen* tasks. Total counts for each of these 8 sources were extracted in the 0.2–8.0 keV region. Of these 8 sources, only 2 sources have counts greater than 100, suitable for a reasonable spectral analysis. Therefore, for these 2 sources, spectra were grouped in 15 counts/bin and taken into XSPEC (Arnaud 1996) for spectral analysis. We performed the fit by minimizing χ^2 . We model the spectra as a single power law continuum emission with absorption. The observed and fitted spectra are shown in Fig. 12. For both sources, N_{H} values are found to be less than 10^{22} cm^{-2} and similar to the Galactic values. Similar conclusion was found by Giustini et al. (2008) when they fitted the spectra of their BAL sample assuming neutral absorbers. Recently, Streblyanska et al. (2010) found that about 36% of their sample of BALs have low N_{H} when the spectra are fitted with a model including a neutral absorber. However, when the spectra are modeled with an ionized absorber, Streblyanska et al. (2010) found high values of N_{H} for more than 90% of their sources. Due to the low count rates of the objects we study here, we are unable to apply such detailed models. Therefore, the N_{H} values reported here for the two X-ray brightest objects in our sample should be treated as lower limits. For our two sources, we found a photon index Γ values, 1.62 ± 0.44 and 2.80 ± 0.89 , which is similar to that of typical radio-quiet quasars (Piconcelli et al. 2005) and within error of the mean photon index, $\Gamma = 1.87 \pm 0.21$, found from spectral analysis of 22 BAL quasars by Giustini et al. (2008). The results of our X-ray analysis on the 8 BAL quasars are summarized in Table 3.

5 CONCLUSION

We have presented a new sample of 16 BAL quasars selected from a homogeneous sample of 159 $z_{\text{em}} > 1.5$, $g' < 22$ mag quasars found in a region of CFHTLS overlapping with the XMM-LSS and SWIRE surveys.

(i) We find a BAL quasar fraction of $\sim 10\%$ in the whole sample and of $\sim 8\%$ among optically selected quasars (120 quasars). This is similar to what is found from other optically selected quasar samples (Weymann et al. 1991; Hewett & Foltz 2003; Trump et al. 2006; Knigge et al. 2008; Gibson et al. 2009). Also, 7% of the XMM selected quasars are found to be BAL quasars. If we consider the 12 quasars which were selected from SWIRE colours only (and rejected by the optical colour selection), 4 are found to be BAL quasars which gives a BAL fraction of $\sim 33\%$. This agrees with the large 23% BAL quasar fraction found in 2MASS selected quasars by Dai et al. (2008). We note here that recently Allen et al. (2010), after correcting for selection biases, report an intrinsic C IV BAL quasar fraction of $\sim 41 \pm 5$ per cent, though their observed fraction is 8.0 ± 0.1 per cent.

(ii) The values of $\Delta\alpha_{\text{ox}}$, the deviation of the spectral index, α_{ox} , from the mean in the overall sample at the same UV luminosity, are distributed symmetrically around zero, whereas the $\Delta\alpha_{\text{ox}}$ values of XMM detected BAL quasars are shifted towards lower values with an average of -0.169 ± 0.161 . This shows that the X-ray detected BAL quasars are weaker than the X-ray detected non-BAL quasars by a factor of about 3. This X-ray weakness of BAL quasars compared to non-BAL quasars is similar to what was found in earlier studies (G06; Fan et al. 2009; Gibson et al. 2009) however, contrasts with the results of Giustini et al. (2008). The discrepancy we find is however much less than what was reported by G06 who found that optically bright BAL quasars, are X-ray sources weaker by a factor of 30 compared to non-BAL quasars. This might be due to the fact that G06 had used *Chandra* observations reaching significantly fainter flux levels than the XMM-Newton observations used here for our sample of BALs.

(iii) We investigated various correlations between the properties of the C IV absorptions and α_{ox} using an extended sample gathered after combining our data with those of Gallagher et al. (2006), Giustini et al. (2008), Gibson et al. (2009) and Fan et al. (2009). For this large HiBAL quasar sample, $\Delta\alpha_{\text{ox}}$ was calculated and we find it to be correlated with the balnicity index, BI, and the maximum velocity of the outflow, V_{max} . Similarly, V_{max} and BI are correlated with the 2500 Å monochromatic luminosity, $L_{2500\text{\AA}}$. This suggests that quasars with high velocity outflows are X-ray weak. While there is a large range in V_{max} , for a given $L_{2500\text{\AA}}$ at $\log(L_{2500\text{\AA}}) < 31$, there is a lack of objects with $V_{\text{max}} < 10^4$ km/s at the high luminosity end. Thus there seems to be a lower envelope, the presence of which dominates the above correlation. This probably means that even if radiation pressure is the main driver of the flow, other parameters are important such as the launching radius, the shape of the ionizing spectrum, the mass of the wind, the properties of the confining medium, etc.

(iv) We find the mean X-ray hardness ratio, HR, of XMM detected non-BAL and BAL quasars to be -0.61 ± 0.20 and -0.49 ± 0.20 respectively. While this is consistent with the

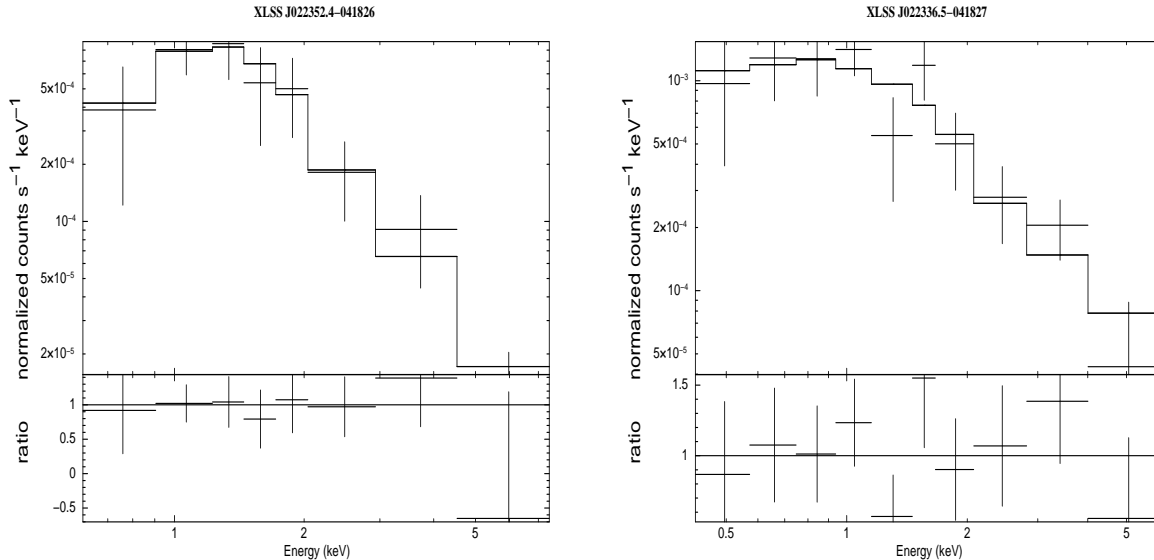


Figure 12. The observed and the fitted spectra of the two XMM detected BAL quasars with counts larger than 100.

Table 3. X-ray spectral properties of the XMM detected BAL quasars. Column 1 is the XMM name, column 2 is the XMM observation ID, column 3 is the hardness ratio measured between 0.2–2.0 keV and 2.0–12.0 keV, column 4 is the Galactic neutral column density derived from Dickey & Lockman (1990), column 5 is the neutral column density from the spectral fit and last column gives the fitted photon spectral index

Name	ObsID	HR	$N_{\text{H,Gal}} (10^{20})$ cm^{-2}	$N_{\text{H}} (10^{20})$ cm^{-2}	Γ
XLSS J022302.3-044437	0109520501	0.63 ± 1.09	2.68		
XLSS J022352.4-041826	0210490101	-0.52 ± 0.17	2.54	6.04 ± 0.33	2.80 ± 0.89
XLSS J022624.7-040458	0112680201	-0.28 ± 0.33	2.65		
XLSS J022647.7-041426	0112680101	-0.33 ± 0.27	2.66		
XLSS J022645.4-043615	0112681301	-0.41 ± 0.23	2.46		
XLSS J022257.2-042953	0109520601	-0.50 ± 0.55	2.63		
XLSS J022132.9-043750	0112680801	-0.90 ± 0.59	2.58		
XLSS J022336.5-041827	0210490101	-0.45 ± 0.10	2.55	0.97 ± 0.11	1.62 ± 0.44

assumption that the X-ray weakness is due to soft X-ray absorption, the number of X-ray detected BAL quasars is too small to make any statistically significant claim.

(v) The fit of the X-ray spectra from two BAL quasars shows that they have neutral hydrogen column densities smaller than 10^{22} cm^{-2} and close to the Galactic values. This is based on a fully covering neutral absorber model. However, if the absorber is ionized and/or partially covering the X-ray source, the column density derived for these two BAL quasars should be considered lower limits. For these two BAL quasars, the photon spectral index is found to be similar to that of radio-quiet quasars. This agrees with the photon index values found recently from X-ray spectral analysis of a larger sample of BAL quasars (Giustini et al. 2008; Streblyanska et al. 2010).

ACKNOWLEDGMENTS

We thank the anonymous referees for their valuable comments which helped to significantly improve the paper. We

also thank all the present and former staff of the Anglo-Australian Observatory for their work in building and operating the AAOmega facility. This work used the CFHTLS data products, which is based on observations obtained with MegaPrime/MegaCam, a joint project of CFHT and CEA/DAPNIA, at the Canada-France-Hawaii Telescope (CFHT) which is operated by the National Research Council (NRC) of Canada, the Institut National des Science de l’Univers of the Centre National de la Recherche Scientifique (CNRS) of France, and the University of Hawaii. This work is based in part on data products produced at TERAPIX and the Canadian Astronomy Data Center as part of the Canada-France-Hawaii Telescope Legacy Survey, a collaborative project of NRC and CNRS.

REFERENCES

- Allen, J. T., Hewett, P. C., Maddox, N., Richards, G. T., Belokurov, V. 2010, *MNRAS in press*
 Anderson et al. 2007, *AJ*, 133, 313
 Arav N., Li Z-Y., Begelman M.C., 1994, *ApJ*, 432, 62

- Arnaud K.A., 1996 in ASP Conf. Series, Vol. 101, *Astronomical Data Analysis Software and Systems V.* ed. G. H. Jacoby & J. Barnes, 17
- Becker R. H., White R. L., Gregg M. D., Brotherton M. S., Laurent-Muehleisen S. A., Arav N., 2000, *ApJ*, 538, 72
- Bolzonnella M., Miralles J. M., Pellò R., 2000, *A&A*, 363, 476
- Brotherton M.S., Laurent-Muehleisen S. A., Becker R. H., Gregg M. D., Telis G., White R. L., Shang Z., 2005, *AJ*, 130, 2006
- Dai X., Shankar F., Sivakoff G. R., 2008, *ApJ*, 672, 108
- Dickey J. M., Lockman F. J., 1990, *ARA&A*, 28, 385
- DiPompeo M. A., Brotherton M. S., Becker R. H., Tran H. D., Gregg M. D., White R. L., Laurent-Muehleisen S. A., 2010, *ApJS*, 189, 83
- Fan L. L., Wang H. Y., Wang T., Wang J., Dong X., Zhang K., Cheng F., 2009, *ApJ*, 690, 1006
- Gallagher S.C., Brandt W. N., Chartas G., Garmire G. P., 2002, *ApJ*, 567, 37
- Gallagher S.C., Brandt W. N., Chartas G., Priddey R., Garmire G. P., Sambruna R. M., 2006, *ApJ*, 644, 709 (G06)
- Gallagher S. C., Hines D. C., Blaylock M., Priddey R. S., Brandt W. N., Egami E. E., 2007, *ApJ*, 665, 157
- Ganguly R., Brotherton M. S., Cales S., Scoggins B., Shang Z., Vestergaard M., 2007, *ApJ*, 665, 990
- Ghosh K.K., Punsly B., 2008, *ApJL*, 674, 69
- Gibson R., et al. 2009, *ApJ*, 692, 758
- Giustini M., Cappi M., Vignali C., 2008, *A&A*, 491, 425
- Goodrich R. W., Miller J. S., 1995, *ApJL*, 448, 73
- Green P.J., et al. 1995, *ApJ*, 405, 51
- Green P.J., Mathur S., 1996, *ApJ*, 462, 637
- Green P.J., et al. 2001, *ApJ*, 558, 109
- Green P.J., et al. 2009, *ApJ*, 690, 644
- Gupta N., Srianand R., Petitjean P., Ledoux C., 2003, *A&A*, 406, 65
- Hazard C., Morton D. C., Terlevich R., McMohan R., 1984, *ApJ*, 282, 33
- Hewett P. C., Foltz C. B., 2003, *AJ*, 125, 1784
- Hines D. C., Wills B. J., 1995, *ApJL*, 448, 69
- Hutsemekers D., Lamy H., Remy M., 1998, *A&A*, 340, 371
- Just D.W., Brandt W. N., Shemmer O., Steffen A. T., Schneider D. P., Chartas G., Garmire G. P., 2007, *ApJ*, 665, 1004
- Knigge C., Scaringi S., Goad M. R., Cottis C. E., 2008, *MNRAS*, 386, 1426
- Laor et al. 1997, *ApJ*, 477, 93
- Laor A., Brandt W. N., 2002, *ApJ*, 569, 641
- Lavalley M., Isobe T., Feigelson E., 1992, in ASP Conf. Series, 25, *Astronomical Data Analysis Software and Systems - I*, eds. D. M. Worall, C. Biemesderfer & J. Barnes, p. 245
- Lonsdale et al. 2003, *PASP*, 115, 897
- Mathur S. et al. 2000, *ApJL*, 533, 79
- Miller B. P., Brandt W. N., Gibson R. R., Garmire G. P., Shemmer O., 2009, *ApJ*, 702, 911
- Murray, N., & Chiang, J. 1995, *ApJL*, 454, 105
- Oke J.B., Gunn J.E., 1983, *ApJ*, 266, 713
- Piconcelli E., Jimenez-Bailón E., Guainazzi M., Schartel N., Rodríguez-Pascual P. M., Santos-Lleó M., 2005, *A&A*, 432, 15
- Pierre M., et al. 2004 *JCAP*, 09, 011
- Pierre M., et al. 2007, *MNRAS*, 382, 279
- Priddey R. S., Gallagher S. C., Issak K. G., Sharp R. G., McMohan R. G., Butner H. M., 2007, *MNRAS* 374, 867
- Proga D., Stone J. M., Kallman T. R., 2000, 543, 686
- Reichard et al. 2003, *AJ*, 126, 2594
- Richards, G.T., et al. 2002, *AJ*, 123, 2945
- Sabra B. M., Hamann F., 2001, *ApJ*, 563, 555
- Schmidt G.D., Hines D.C., 1999, *ApJ*, 512, 125
- Shankar F., Dai X., Sivakoff G. R., 2008, *ApJ*, 687, 859
- Sharp R., et al. 2006, in McLean I.S., Iye M., eds, *Proceedings of the SPIE*, Vol. 6269, *Ground-based and Airborne Instrumentation for Astronomy* (astro-ph/0606137)
- Sprayberry D., Foltz C. B., 1992, *ApJ*, 390, 39
- Srianand R., Petitjean P., 2000, *A&A*, 357, 414
- Srianand R., Petitjean P., Ledoux C., Hazard C., 2002, *MNRAS*, 336, 753
- Stalin, C. S., Petitjean P., Srianand R., Fox A. J., Coppolani F., Schwobe A., 2010, *MNRAS*, 401, 294
- Steffen A. T. et al. 2006, *AJ*, 131, 2826
- Stern D., Djorgovski S. G., Perley R. A., de Carvalho R. R., Wall J. V., 2000, *AJ*, 119, 1526
- Stern D., et al. 2005, *ApJ*, 631, 163
- Streblyanska A., Barcons X., Carrera F.J., Gil-Merino R., 2010, *A&A*, 515, 2
- Tolea A., Krolik J. H., Tsvetanov Z., 2002, *ApJ*, 578, 31
- Trump J. R., 2006, *ApJS*, 165, 1
- Urrutia T., Becker R. H., White R. L., Glikman E., Lacy M., Hodge J., Gregg M. D., 2009, *ApJ*, 698, 1095
- Wampler E. J., Chugai N. N., Petitjean P., 1995, *ApJ*, 443, 586
- Wang J., Jiang P., Zhou H., Wang T., Dong X., Wang H., 2008, *ApJL*, 676, 97
- Weymann R.J., et al. 1991, *ApJ*, 373, 23
- Willott C., Rawlings S., Grimes J.A., 2003, *ApJ*, 598, 909

